Membrane Binding of Twin Arginine Preproteins as an Early Step in Translocation

Anitha Shanmugham, Harro W. Wong Fong Sang, Yves J. M. Bollen, and Holger Lill*

Institute of Molecular Cell Biology, Department of Structural Biology, Vrije Universiteit, De Boelelaan 1087, 1081 HV Amsterdam, The Netherlands

Received October 26, 2005; Revised Manuscript Received December 16, 2005

ABSTRACT: The twin arginine transport (Tat) system translocates folded proteins across the bacterial inner membrane. Transport substrates are recognized by means of evolutionarily well-conserved N-terminal signal peptides. The precise role of signal peptides in the actual transport process is not yet fully understood. Potentially, much insight into the molecular details of the transport process could be gained from step-by-step in vitro experiments under controlled conditions. Here, we employ purified preproteins to study their interaction with the phospholipid membrane by using surface plasmon resonance spectroscopy. It turns out that preproteins interact tightly with a model membrane consisting of only phospholipids. This interaction, which is stabilized by both electrostatic and hydrophobic contributions, appears to constitute an early step in protein translocation by the Tat system.

Transport of proteins across membranes is a crucial problem for every living cell. In prokaryotes, two different protein complexes have been found engaged in this task. One is the long-known and well-addressed general secretory (Sec)[1] transport system. Sec translocons open narrow pores and transport largely unfolded proteins into the bacterial periplasmic space (*1*), where they eventually fold and become active. On the other hand, the rather recently discovered twin arginine transport (Tat) system translocates folded proteins across the bacterial inner membrane, often incorporating large cofactors or even present in a multimeric state (*2*). Consequently, pores opened by this complex need to be of variable size, up to 100 Å in diameter, and the transport process is expected to be very different from the one employed by Sec.

Despite these differences, the two transport systems do have features in common. Transport substrates of either route are identified by means of so-called signal peptides. Signal peptides are evolutionarily well-conserved N-terminal extensions and comprise three distinct regions (Figure 1). The n-region often harbors positive charges. The subsequent h-region has a rather hydrophobic character. A final c-region is terminated by a signal peptidase cleavage site, which is utilized to remove the signal peptide during transport (*3*). Despite overall conservation, signal peptides found in Tat substrates do have several distinguishing features as compared to those found in Sec substrates. Their n-region is generally much longer. On the boundary between the n- and h-regions, signal peptides found in Tat substrates contain the name-giving twin arginine motif, S/TRRxFxK. The h-regions in Tat signal peptides are often somewhat longer but exhibit generally reduced hydrophobicity. An additional lysine or arginine is often present in the c-regions of Tat signal peptides.

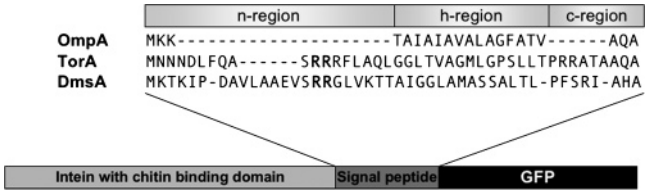

FIGURE 1: Representation of the expression region of the pTYB11 constructs. The intein tag is fused to the N-terminus of the signal peptide region of the preprotein (signal−GFP) for expression in *E. coli* BL21(DE3)* cells. The signal peptides of the Sec substrate OmpA and the Tat substrates TorA and DmsA are tentatively aligned in the zoom according to the three conserved regions. The name-giving arginine pairs are represented in bold.

The precise role of signal peptides in the actual transport process is not yet fully understood. It seems clear that Sec signals interact with several constituents of the transport machinery. Also, interaction with several cytosolic proteins was shown to be essential for correct targeting of Sec substrates (*4*). Furthermore, the presence of a distinctly hydrophobic region has sparked the idea that there might be a more general interaction of signal peptides with biological membranes prior to or during transport. With synthetic Sec signal peptides, which were not coupled to substrates, such interactions have indeed been demonstrated (*5*−*7*). The significance of these findings for the in vivo situation is not entirely clear; cytosolic targeting factors such as SecA and SecB may prevent membrane interaction of Sec signal peptides. In contrast, no general cytosolic targeting factors are known to be involved in targeting of Tat substrates (see, e.g., ref *8*). Membrane interaction of Tat substrates thus may well be relevant in vivo. Indeed, several lines of evidence point in this direction. For example, it is shown that translocation of proteins through the Tat pathway depends on the presence of anionic phospholipids and on lipid polymorphism much more strongly than Sec-mediated translocation (*9*). Furthermore, Tat preproteins are found bound to the membrane of a ΔTat mutant strain (*8*). However, direct interaction of Tat signals with membranes has not yet been explicitly investigated.

* To whom correspondence should be addressed. Phone: +31 20 5987164. Fax: +31 20 5987136. E-mail: holger.lill@falw.vu.nl.

[1] Abbreviations: CL, cardiolipin; GFP, green fluorescent protein; Sec, general secretory pathway; SPR, surface plasmon resonance; Tat, twin arginine translocation pathway; PE, L-α-phosphatidylethanolamine; PG, L-α-phosphatidylglycerol.

10.1021/bi052188a CCC: $33.50
Published on Web 01/31/2006

To further unravel the underlying processes, in vitro examination of single events during transport comprises the logical next step. Such studies have been hampered so far by the unavailability of purified transport-competent preproteins. Here, we describe a general strategy for the production of transport-competent substrates. A self-cleaving N-terminal tag is introduced to allow chromatographic purification but even more importantly to cap and protect the signal during expression and purification. We use this strategy to produce artificial substrates based on the green fluorescent protein (GFP) fused to different signal peptides. Integral preproteins produced by this method have then been utilized to monitor interactions with membranes by means of surface plasmon resonance spectroscopy. It turned out that signal peptides mediate the firm attachment of substrates to a membrane. This could constitute a first event en route to transport, thereby reducing the stage for all following processes to two dimensions, which might potentially accelerate transport (*10*).

MATERIALS AND METHODS

Bacterial Strains, Genes, and Plasmids. Vector pTYB11 (New England Biolabs) has been used to fuse a cleavable 55 kDa intein tag to various signal peptides and then to GFP (Figure 1). The signal peptides originated from trimethylamine *N*-oxide reductase A (TorA), from dimethyl sulfoxide reductase A (DmsA), and from outer membrane protein A (OmpA). The fusion proteins were expressed in *Escherichia coli* BL21(DE3)* cells.

As first shown in ref *11*, the *E. coli tat* operon cloned into a plasmid functionally complements Tat activity in *E. coli* tat mutant cells. In this study, we employed plasmid pCS553 (C. Sanders, unpublished results), which uses a *tac* promoter to control moderate overexpression of the complete *E. coli tat* operon, in *E. coli* strain MC4100. Complementation of Tat activity in Δ*tat* mutant strain DADE (*12*) has been reconfirmed (A. Shanmugham, unpublished observations).

Expression and Purification of Export-Competent Signal GFPs. For translocation assays, the intein-fused GFPs were expressed in *E. coli* MC4100 and DADE cells. For large-scale purification, the intein-fused signal GFPs were expressed in *E. coli* BL21(DE3)* cells and column purified as described in the IMPACT-CN system manual (New England Biolabs). Upon addition of DTT, the intein moiety underwent specific self-cleavage from the signal GFPs. Whereas intein itself remained bound to the chitin beads of the column, signal GFPs were eluted and subjected to N-terminal sequencing (Eurosequence, Groningen, The Netherlands).

Isolation of Periplasmic Proteins. We extracted periplasmic proteins from cells expressing the different intein-fused signal GFPs by combining the lysozymal action of cell wall lysis with osmotic shock, as described in ref *13*. Both the spheroplasts and the periplasmic samples were heat denatured (95 °C for 10 min) in loading buffer without any reducing agent and analyzed via 12% SDS−PAGE. The proteins in the gel were immobilized on a nitrocellulose membrane, and the cellular localization of GFP was analyzed by immunoblotting, using antibodies to GFP (Biotrend).

Fluorescence Measurements. Fluorescence intensities of cells and of periplasmic extracts were recorded on a Cary Eclipse fluorescence spectrometer (excitation at 480 nm, emission at 508 nm, 300 μL sample volume, 96-well plate reader, 25 °C).

Preparation of Model Lipid Layers. Lipids mimicking the *E. coli* inner membrane composition (*14*) [70:25:5 mixture of L-α-phosphatidylethanolamine (PE), L-α-phosphatidylglycerol (PG), and cardiolipin (CL), all from Sigma] were solubilized at 2 mg/mL in a 2:1 mixture of chloroform and methanol. Small unilamellar vesicles (SUVs) were generated from this mixture as described in ref *15*. SUVs were finally suspended in HBS buffer [10 mM Hepes (pH 7.5), 150 mM NaCl, and 3 mM EDTA] and extruded 10 times through a polycarbonate membrane with 200 nm pores (Avestin). In one experiment, the number of negatively charged headgroups was varied by changing the percentage of negative PG between 5 and 70%. The change in PG content was compensated by the amount of PE; the percentage of CL was kept constant at 5%. SUVs were spread and immobilized on L1 sensor chips (Biacore AB). The L1 chip surface contains hydrophobic aliphatic chains covalently linked to a dextran-coated gold surface and promotes the formation of bilayers from immobilized SUVs. To remove any multilamellar structures from the lipid surface, we injected after layer formation 50 μL of 5 mM NaOH; 25 μL of a BSA solution (0.1 mg/μL in HBS buffer) was injected over the chip surface as an indicator for coverage of the chip surface by the bilayer (*15*). After completion of an experiment, the surface of the chip was regenerated by washing with 40 mM *N*-octyl β-D-glucopyranoside.

Preparation of Membrane Layers from Inverted Membrane Vesicles (IMVs). IMVs containing either wild-type levels or overexpression levels (using plasmid pCS553) of TatABC were obtained from *E. coli* MC4100 as described in ref *16*. IMVs were also made from TatABC deletion strain DADE. IMVs [2 mg/mL in 10 mM Hepes (pH 7.6), 150 mM NaCl, 5 mM $MgCl_2$, and 3 mM EDTA] were treated like SUVs with regard to their immobilization on the L1 chip surface, except that the bilayers made from IMVs were not treated with NaOH to prevent potential damage to membrane proteins.

SPR Measurements. SPR measurements were performed on a Biacore 2000 system (Biacore AB, Uppsala, Sweden) using L1 chips at 25 °C. This system has four different flow cells, which allow single or serial flows at a given time. The running buffer was HBS buffer. Furthermore, we used 10−100 mM NaOH and 100 mM Na_2CO_3 for disruption of lipid−protein interactions. All solutions were freshly prepared, degassed, and filtered through 0.22 μm pores. In a Biacore instrument, SPR is used to measure changes in the refractive index that result from the binding of macromolecules to chip surfaces. Changes in the densities on the chip surface are expressed as resonance units (RUs), and when RUs are plotted against time, a response curve called a sensorgram is obtained. These sensorgrams were analyzed by curve fitting using ProFit (Quantumsoft, Zürich, Switzerland).

Size Exclusion Chromatography. Purified signal GFPs in 20 mM Hepes, 180 mM NaCl, and 3 mM EDTA (pH 7.4) were incubated with phospholipid vesicles mimicking the *E. coli* inner membrane composition. After 1 h, the samples were size-separated on pre-equilibrated homemade columns containing 1 mL of Sephadex G-75 resin (Pharmacia,

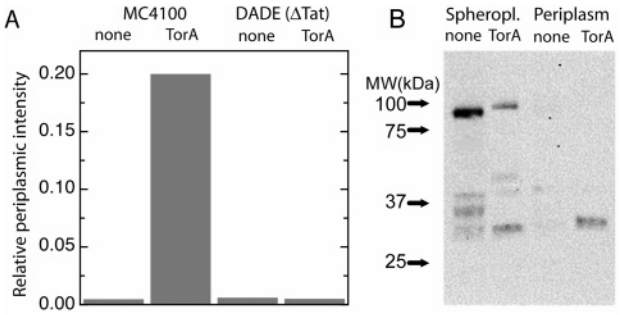

FIGURE 2: GFP molecules with a Tat-specific export signal peptide that lose their intein tag are transported into the periplasm. Fluorescence measurements (A) show that GFP accumulates in the periplasm only when fused to a Tat signal peptide and in the presence of a functional Tat system. Shown is the fraction of the total GFP fluorescence that originates from the periplasm. The *E. coli* strain used (MC4100 or DADE) and the presence or absence of a TorA signal peptide between the intein and the GFP are indicated above the graph. (B) Western blot analysis of the spheroplast and periplasmic fractions of BL21 cells expressing intein fused to GFP with and without a TorA signal peptide. In the spheroplasts, GFP is found as an intein fusion (81 or 85 kDa), as free GFP (30 kDa), and as a number of states with intermediate apparent sizes. GFP is only detected in the periplasm when expressed with a TorA signal peptide. The apparent size of these GFP molecules corresponds to GFP deprived of both the intein tag and signal peptide.

Uppsala, Sweden). The presence of GFP in the vesicles, which elute in the first fraction, was detected with fluorescence measurements. GFP without the signal peptide was used as a control.

RESULTS

Overproduction of Preproteins. Green fluorescent protein (GFP) was genetically fused behind the signal peptides of TorA and DmsA, both genuine Tat substrates, and of OmpA, a Sec substrate (see Materials and Methods). These signal GFPs were then fused behind an intein. Inteins are proteins that remove themselves from fusion proteins by means of cleavage under reducing conditions. Using the intein-mediated protein purification strategy (see Materials and Methods), 5 mg each of purified TorA−GFP and DmsA−GFP fusions and 3 mg of OmpA−GFP fusion were obtained from 1 L of culture volume. After removal of the intein tag, N-terminal sequencing of these samples revealed intact N-termini of the signal peptide regions. Obviously, signal peptides were protected against proteolytic digestion by the N-terminal intein tag. Also, all of the samples displayed fluorescence, indicating that GFP was correctly folded.

Ideally, removal of intein should be triggered exclusively by changing redox conditions during protein purification. However, to some extent the respective redox reaction does also happen spontaneously in cells, which would result in the release of signal GFPs. To verify export competence of this splicing product, the cells were fractionated into spheroplasts and periplasmic extracts. GFP fluorescence was detected in the periplasmic fractions isolated from cells expressing the intein−TorA−GFP fusion. No such fluorescence was found upon expression of intein−GFP fusions missing any signal peptide (Figure 2A). In DADE cells, which lack the entire Tat operon, no GFP fluorescence could be detected in periplasm irrespective of the presence of a TorA signal peptide (Figure 2A). As inferred from Western blots, GFP molecules found in periplasmic fractions had a size which corresponds to GFP deprived of their intein tags as well as of signal peptides (Figure 2B). For the intein−DmsA−GFP fusion, similar results were obtained as described for the intein−TorA−GFP fusion (not shown). We interpret these findings as being a result of Tat-mediated transport of signal GFPs that have lost their capping intein and thereby as an inherent proof for transport competence. Note the absence of intein-fused GFP in the periplasmic fractions, which illustrates the quality of the fractionation.

Preprotein−Membrane Interaction Analysis. First, we performed a crude preprotein−membrane interaction assay. Purified signal GFPs were mixed with phospholipid vesicles mimicking the *E. coli* inner membrane lipid composition (70:25:5 PE/PG/CL mixture). The samples were then size-separated on a Sephadex G-75 column. Fluorescence measurements revealed that all three signal GFPs (i.e., TorA−GFP, DmsA−GFP, and OmpA−GFP fusions) eluted with the phospholipid vesicles (not shown). GFP without a signal peptide did not elute with the vesicles, which indicates that signal GFPs bind to phospholipid membranes.

We investigated this preprotein−membrane interaction in more detail by using SPR spectroscopy. Phospholipid bilayers mimicking the *E. coli* inner membrane lipid composition have been spread onto a L1 chip as described in Materials and Methods. Purified preproteins (each 50 nM) were exposed individually to this surface for a time period of 90 s. Figure 3A depicts typical SPR raw data as obtained with signal-free GFP. Upon protein injection, a stepwise increase in the magnitude of the signal (light gray) was observed. After a switch to GFP-free buffer was made, this increase reversed in another timely unresolved step to nearly the original level. Such signals are typically not due to any interaction of the protein with the surface but rather reflect different refractive indices of buffers with or without protein.

In contrast to signal-free GFP, which did not show any stable interaction with the bilayer, all signal GFPs did bind to the artificial membrane (Figure 3A). Binding characteristics were highly variable among the various preproteins. The OmpA−GFP fusion associated rather slowly with the membrane, whereas TorA− and DmsA−GFP fusions displayed much faster association kinetics. To gain further insight into the preprotein−lipid interaction, binding curves of the TorA−GFP fusion were generated at a range of protein concentrations (from 25 to 100 nM). Single exponentials could be fitted to those parts of the response curves that reflect association with phospholipid bilayers. As exemplified for the TorA−GFP fusion in Figure 3B, the resulting rate constants increased linearly with protein concentration, yielding with the TorA signal a second-order binding constant of $(3.55 \pm 0.01) \times 10^5\ s^{-1}\ M^{-1}$ (Figure 3B).

After removal of the unbound protein, the GFP bearing the OmpA signal peptide did not dissociate substantially in the time course of observation. With TorA−GFP and DmsA−GFP fusions, approximately two-thirds of the bound molecules dissociated from the membrane in a kinetically resolved manner, whereas one-third remained bound. The dissociation kinetics turned out to be complex and have not been analyzed quantitatively. Qualitatively, this observation suggests that GFP bearing a Tat signal peptide binds to the lipid bilayer in at least two different modes: one weakly bound and one more tightly bound.

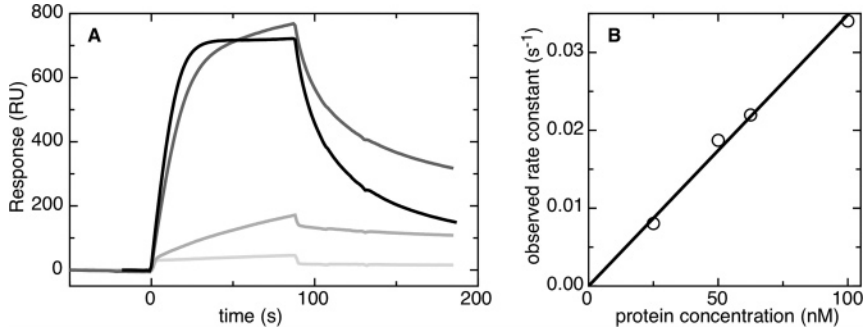

FIGURE 3: GFP preproteins interact with phospholipid bilayers. (A) Raw SPR data obtained with (from light to dark) signal-free GFP and OmpA−GFP, DmsA−GFP, and TorA−GFP fusions. Upon protein injection of signal-free GFP, the SPR-signal rises stepwise. After the switch to GFP-free buffer is made (90 s after injection), the signal drops back almost to the original level. This stepwise behavior is caused by different refractive indices of buffers with or without protein. In contrast, the response curves for the different signal−GFP fusions rise in a time-resolved manner. Clearly, signal−GFP fusions interact with the model phospholipid bilayer (see Materials and Methods for details on its composition). Association of signal−GFP fusions with the bilayer is monoexponential. After the switch to GFP-free buffer is made, the bound signal−GFP fusions partly dissociate from the surface. (B) The rate at which the signal−GFP fusion binds to the bilayer increases linearly with protein concentration. In the case of the TorA−GFP fusion, the resulting second-order rate constant is 3.55×10^5 s^{-1} M^{-1}.

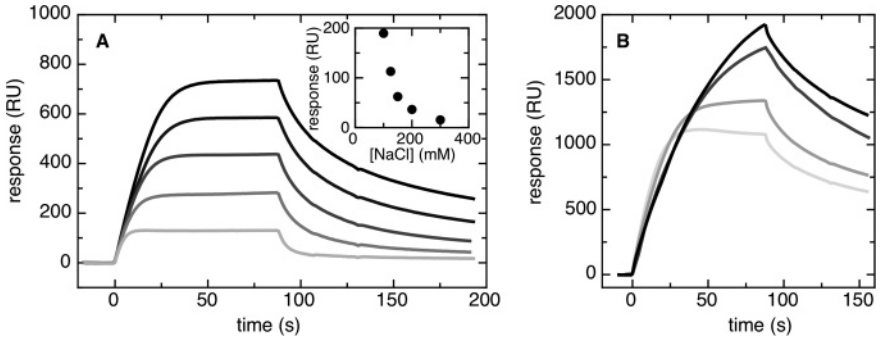

FIGURE 4: Association of the TorA−GFP fusion with a phospholipid bilayer is dominated by electrostatic attraction. (A) SPR response curves for the binding of the TorA−GFP fusion to a phospholipid bilayer in the presence of (from dark to light) 100, 125, 150, 200, and 300 mM NaCl. The increasing salt concentration clearly reduces the amount of preprotein that binds during the 90 s association phase. The inset shows that the amount of preprotein that remains bound after dissociation is also reduced with an increase in salt concentration. In the presence of 300 mM NaCl, virtually no preprotein binds to the bilayer. (B) Reducing the amount of negatively charged PG in the bilayer also reduces the amount of preprotein that binds to it. Depicted are SPR response curves for binding of the TorA−GFP fusion to phospholipid bilayers that contain (from light to dark) 5, 15, 50, or 70% PG (see Materials and Methods for details on the composition of the bilayer).

Binding Stability. To check the contribution of electrostatic forces to preprotein−lipid interaction, binding experiments have been performed in the presence of various salt concentrations. Figure 4A shows that increasing concentrations of shielding ions decrease both the amount of protein that binds during injection and the amount of protein that remains bound after dissociation for 100 s. These results, which correspond to electrostatic interaction theory (*17*), show that electrostatic forces play an important role in the preprotein−lipid interaction at physiological ionic strength [equivalent to 170−240 mM salt (*18*)].

The electrostatic interaction described above is most likely due to the positive charges on the signal peptide and negative charges on the *E. coli* inner membrane. To further substantiate this finding, we varied the density of negative charges on the bilayer surface (Figure 4B). The experiment demonstrates a largely weakened binding of preproteins to less densely charged layers. Association kinetics on this surface are complex, which hampers a detailed quantitative analysis of these data. Still, this result confirms the previous conclusion that electrostatic interaction is important in stabilizing the preprotein−lipid complex.

Part of the TorA−GFP and DmsA−GFP molecules and virtually all of the OmpA−GFP molecules remain tightly bound to the phospholipid bilayer upon removal of unbound protein. The stability of these preprotein−lipid complexes has been addressed by washing the surfaces with buffers commonly used for disruption of protein−membrane interactions. The results of washing with high-salt buffer (300 mM NaCl in HBS buffer, wash 1) and carbonate buffer (100 mM Na_2CO_3 at pH 11, wash 2) are exemplified for the TorA−GFP fusion in Figure 5. The data indicate that in these buffers, no substantial amount of membrane-bound TorA−GFP fusion was released. Finally, we used a 100 mM NaOH solution (Figure 5, wash 3), which damages the lipid bilayer structure and hence disrupts any protein−lipid interaction. Accordingly, this treatment significantly decreased the amount of bound protein.

The results described above show that preproteins that do not spontaneously dissociate from the phospholipid bilayer can also not be removed by high salt or pH, suggesting that these preprotein−bilayer complexes are stabilized by more than electrostatic forces alone.

Interaction of the Preprotein with Native Membranes. An obvious question that arose during this study was how the in vitro-detected interactions compare to the in vivo situation. One possibility was that within cells, interactions of the preprotein with protein complexes present in *E. coli* inner membranes could simply overrule the ones examined here. We have therefore prepared membrane bilayer surfaces from

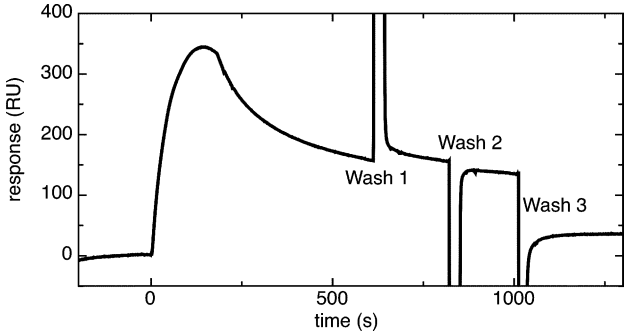

FIGURE 5: Part of TorA−GFP preproteins that bind tightly to a phospholipid bilayer. At time zero, the TorA−GFP fusion is injected over a phospholipid bilayer (PE/PG/CL; see Materials and Methods). Washing with GFP-free buffer (starting at 180 s) releases part of the bound preproteins. Subsequent washes with 300 mM NaCl in HBS buffer (wash 1) and carbonate buffer (wash 2) do not remove any substantial amounts of membrane-bound TorA−GFP fusion. A harsh treatment (100 mM NaOH, wash 3) is needed to remove the tightly bound preproteins.

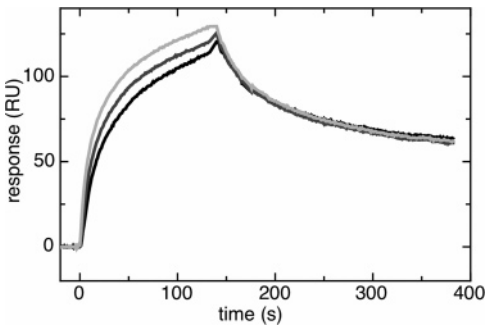

FIGURE 6: Binding of the TorA−GFP fusion to cytoplasmic *E. coli* membranes. TorA−GFP is injected separately over natural bilayers from inverted inner membrane vesicles of *E. coli* MC4100 cells overexpressing the Tat compounds (black curve), of wild-type *E. coli* MC4100 cells (dark gray curve), and of Δ*tat* mutant *E. coli* DADE cells (light gray curve) for a time period of 135 s.

inverted inner membrane vesicles (IMVs) obtained from different *E. coli* strains: *E. coli* DADE cells that are devoid of Tat complexes, wild-type cells with a normal level of translocase subunits, and TatABC-overproducing cells harboring plasmid pCS553. As detailed in Materials and Methods, IMVs of the various strains were adsorbed onto the L1 sensor chip in flow cells 1−3. The TorA−GFP preprotein was injected serially over these membranes from flow cell 1 to 3. The resulting sensorgrams are shown in Figure 6. The magnitude of the response following binding of the TorA−GFP fusion to the biological membrane is small compared to that for binding of the same protein to model membranes (see Figure 3A or 4A). This is caused by two effects. First, IMVs of biological membranes bind less well to the L1 surface by approximately 35%. Second, biological membranes contain a large amount of proteins, which probably further reduces the amount of phospholipids on the SPR surface. It turns out that both the amounts of bound preprotein and the association rates on the three membranes are highly similar. The small differences observed are caused by the order in which the preprotein floats over the different membranes. Due to gradual loss of preprotein by binding, the preprotein concentration is always highest in the first flow cell, containing in this particular experiment a Tat-free membrane, and lowest in the last flow cell, which was loaded here with a membrane originating from the Tat-overproducing strain. The data thus demonstrate that interactions of export-competent Tat preproteins with all of the bacterial membranes used are indistinguishable. This implies that in native membranes, the binding events observed in this study are not overruled by preprotein−Tat complex interactions.

DISCUSSION

Production of Functional Preproteins as a Basis for in Vitro Studies. In general, protein translocation across the bacterial inner membrane is a highly complex and dynamic process. It involves among other constituents preproteins, highly multimeric translocase complexes, and a leader peptidase. Further, hitherto unknown participants might still await discovery. Also, the translocation process itself is far from understood. Potentially, much insight could be gained from step-by-step in vitro experiments under controlled conditions. Such experiments were up to now severely hampered by the fact that export-competent preproteins are difficult to isolate, mainly because of proteolytic digestion (see, e.g., Figure 2B) and unwanted interaction with translocases during expression and purification (*19*). As a consequence, in vitro studies have up to now mainly been limited to synthetic signal peptides.

GFP, which is readily and firmly folded upon expression in *E. coli* and then displays bright fluorescence, has previously been employed as an artificial substrate for the *E. coli* Tat system in in vivo studies (*20*, *21*). Therefore, the observation that preproteins after accidental loss of the intein tag were transported into the periplasmic space came as no surprise. In general, N-terminal fusion of an intein tag to preproteins was found to prevent export as well as degradation of the adjacent signal peptide region. As a result, signal GFPs fused with self-cleavable tags become concentrated in the cytosolic compartment, which enables large-scale purification of intact preproteins and thus detailed and stepwise in vitro examination of transport processes.

Transport Signal Peptides Interact with Phospholipids. As a first inroad to in vitro examination of Tat-mediated protein transport, we studied interaction of the purified artificial substrates with the phospholipid membrane in real time. We chose to use SPR spectroscopy, since this technique enables the determination of binding constants, association rates, and dissociation rates under nativelike conditions. Membrane interaction had been reported before for synthetic, substrate-free Sec-specific signal peptides (*5*−*7*). In a recent review, Brüser and Sanders (*22*) picked up this concept for Tat signal peptides as well and speculated about possible functional consequences of such interactions. It has been shown that thylakoidal Tat substrates strongly interact with membranes in vivo (*23*−*25*). Brüser et al. (*26*) have demonstrated that a Tat substrate originating from *Allochromatium vinosum* did interact with the *E. coli* cytoplasmic membrane and that this interaction was not dependent on the presence of the twin arginine motif or any known Tat components. We have confirmed these findings and examined interactions of signal peptides originating from Sec as well as from Tat substrates with lipid membranes in real time and in vitro. Both types of signal peptides have been shown to mediate association of preproteins with the inner membrane, whereas signal-free GFP did not show any such interaction. Membrane associa-

tion of preproteins could well be an early step in protein translocation by the Sec as well as by the Tat system. However, the slow association kinetics of Sec preproteins with membranes (Figure 3A) allow for competing processes, such as binding to the targeting factor SecB.

As is obvious from the results depicted in Figure 4, screening or reduction of net charged lipids from the bilayer significantly weakened preprotein binding. From this finding, we conclude that attraction of the positively charged n-region by the negatively charged lipid headgroups governs monoexponential association kinetics with a second-order binding constant of $(3.55 \pm 0.01) \times 10^5\ s^{-1}\ M^{-1}$ for the TorA−GFP fusion. But electrostatic interactions alone are not sufficient to explain the partially very tight binding of preproteins as demonstrated in Figure 5. In that experiment, washing membranes with 300 mM NaCl or Na_2CO_3 at pH 11 did not release significant amounts of protein. Note that 300 mM NaCl inhibits binding of the preprotein to the bilayer almost completely, whereas it is unable to remove the preproteins that remain bound after dissociation (compare Figures 4A and 5). This virtual discrepancy can be resolved by assuming that in addition to electrostatic forces, dissociation is also influenced by hydrophobic interactions. We propose that after association, preproteins rearrange on the membrane surface, perhaps by dipping their h-regions into the hydrophobic core. Such a rearrangement would add hydrophobic interactions to the complex. For Sec preproteins, electrostatic as well as hydrophobic interactions with membranes have been postulated (*5*−*7*). The presence of several different binding forces acting in conjunction would also explain our finding that in contrast to association, dissociation is a multiphasic event, indicating the existence of more than one binding mode.

Finally, we scrutinized the significance of our results for the in vivo situation within *E. coli* cells. Membranes with various Tat complex contents were employed in binding experiments, and no differences have been detected in binding patterns with Tat-free or Tat-containing surfaces. This, together with the previous observations that Tat preproteins in vivo bind to the membranes of ΔTat cells (*8*) and that Tat-mediated protein transport depends strongly on membrane composition (*9*), leads us to the conclusion that binding of preproteins to membranes may well constitute a step en route to translocation.

Early Steps in Tat-Mediated Transport. We have summarized our findings and interpretations in the scheme depicted in Figure 7. We propose that interaction of Tat preproteins with the inner membrane is an early step on the path to transport. Our results point toward a major role for electrostatic forces between the positively charged signal peptide region of the preproteins and the anionic lipid headgroups in the association of preproteins with the lipid bilayer. After electrostatic interaction, interaction of the signal peptide's h-region with the apolar environment of the phospholipids is established. This step is likely to induce secondary structure formation within the signal peptide region of the export-competent preprotein (*27*). The different association stages are reflected by multiple phases observed during dissociation of the TorA−GFP fusion from phospholipid bilayers. Overall, we conclude that the preprotein forms an intermediate complex with the inner leaflet of the inner membrane as an early event in Tat transport. The next step

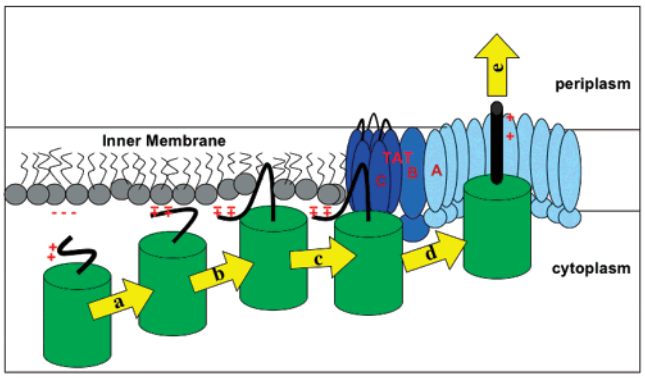

FIGURE 7: Model for the first steps in Tat-mediated protein export. First, the positively charged n-region of the signal peptide interacts with the negative charges on the membrane surface (a). The hydrophobic h-region then dips into the core of the membrane (b). The substrate diffuses laterally through the membrane, until it reaches TatC (c), which leads to the assembly of the Tat pore (d) and translocation of the substrate (e).

in the transport process would then be lateral diffusion of the preprotein along the membrane's surface, which eventually results in binding to the translocase. The preprotein probably first binds to a complex containing TatB and TatC, after which TatA is proposed to be recruited to form the export pore (*2*). Interestingly, the protein transport machinery of the endoplasmic reticulum is shown to be open laterally toward the lipid bilayer (*28*, *29*). Analogously, preproteins might also enter the Tat translocon laterally (Figure 7). This hypothesis remains to be investigated. As a following step in the examination of the transport mechanism of the Tat system, encounters of artificial substrates with the various Tat subunits are currently under investigation.

ACKNOWLEDGMENT

We gratefully acknowledge the contribution of Δ*tat* strain *E. coli* DADE by T. Palmer (Norwich, U.K.). J. W. Borst (Wageningen, The Netherlands) provided the plasmid encoding the intein−GFP fusion.

REFERENCES

1. Pugsley, A. P. (1993) The complete general secretory pathway in Gram-negative bacteria, *Microbiol. Rev. 57*, 50−108.
2. Palmer, T., Sargent, F., and Berks, B. C. (2005) Export of complex cofactor-containing proteins by the bacterial Tat pathway, *Trends Microbiol. 13*, 175−80.
3. Driessen, A. J., Fekkes, P., and van der Wolk, J. P. (1998) The Sec system, *Curr. Opin. Microbiol. 1*, 216−22.
4. Fekkes, P., and Driessen, A. J. (1999) Protein targeting to the bacterial cytoplasmic membrane, *Microbiol. Mol. Biol. Rev. 63*, 161−73.
5. Keller, R. C., ten Berge, D., Nouwen, N., Snel, M. M., Tommassen, J., Marsh, D., and de Kruijff, B. (1996) Mode of insertion of the signal sequence of a bacterial precursor protein into phospholipid bilayers as revealed by cysteine-based site-directed spectroscopy, *Biochemistry 35*, 3063−71.
6. Hoyt, D. W., and Gierasch, L. M. (1991) A peptide corresponding to an export-defective mutant OmpA signal sequence with asparagine in the hydrophobic core is unable to insert into model membranes, *J. Biol. Chem. 266*, 14406−12.
7. Hoyt, D. W., and Gierasch, L. M. (1991) Hydrophobic content and lipid interactions of wild-type and mutant OmpA signal peptides correlate with their in vivo function, *Biochemistry 30*, 10155−63.
8. Ray, N., Oates, J., Turner, R. J., and Robinson, C. (2003) DmsD is required for the biogenesis of DMSO reductase in *Escherichia*

coli but not for the interaction of the DmsA signal peptide with the Tat apparatus, *FEBS Lett. 534*, 156−60.
9. Mikhaleva, N. I., Santini, C. L., Giordano, G., Nesmeyanova, M. A., and Wu, L. F. (1999) Requirement for phospholipids of the translocation of the trimethylamine *N*-oxide reductase through the Tat pathway in *Escherichia coli*, *FEBS Lett. 463*, 331−5.
10. Adam, G., and Delbrück, M. (1968) Reduction of dimensionality in biological diffusion processes, in *Structural Chemistry and Molecular Biology* (Rich, A., and Davidson, N., Eds.) pp 198−215, Freeman, San Francisco.
11. Weiner, J. H., Bilous, P. T., Shaw, G. M., Lubitz, S. P., Frost, L., Thomas, G. H., Cole, J. A., and Turner, R. J. (1998) A novel and ubiquitous system for membrane targeting and secretion of cofactor-containing proteins, *Cell 93*, 93−101.
12. Wexler, M., Sargent, F., Jack, R. L., Stanley, N. R., Bogsch, E. G., Robinson, C., Berks, B. C., and Palmer, T. (2000) TatD is a cytoplasmic protein with DNase activity. No requirement for TatD family proteins in sec-independent protein export, *J. Biol. Chem. 275*, 16717−22.
13. Randall, L. L., and Hardy, S. J. (1986) Correlation of competence for export with lack of tertiary structure of the mature species: A study in vivo of maltose-binding protein in *E. coli*, *Cell 46*, 921−8.
14. Raetz, C. R. (1978) Enzymology, genetics, and regulation of membrane phospholipid synthesis in *Escherichia coli*, *Microbiol. Rev. 42*, 614−59.
15. Erb, E. M., Chen, X., Allen, S., Roberts, C. J., Tendler, S. J., Davies, M. C., and Forsen, S. (2000) Characterization of the surfaces generated by liposome binding to the modified dextran matrix of a surface plasmon resonance sensor chip, *Anal. Biochem. 280*, 29−35.
16. Muller, M., and Blobel, G. (1984) In vitro translocation of bacterial proteins across the plasma membrane of *Escherichia coli*, *Proc. Natl. Acad. Sci. U.S.A. 81*, 7421−5.
17. Stahlberg, J., Jonsson, B., and Horvath, C. (1991) Theory for electrostatic interaction chromatography of proteins, *Anal. Chem. 63*, 1867−74.
18. Kao-Huang, Y., Revzin, A., Butler, A. P., O'Conner, P., Noble, D. W., and von Hippel, P. H. (1977) Nonspecific DNA binding of genome-regulating proteins as a biological control mechanism: Measurement of DNA-bound *Escherichia coli* lac repressor in vivo, *Proc. Natl. Acad. Sci. U.S.A. 74*, 4228−32.
19. Sanders, C., Wethkamp, N., and Lill, H. (2001) Transport of cytochrome *c* derivatives by the bacterial Tat protein translocation system, *Mol. Microbiol. 41*, 241−6.
20. Santini, C. L., Bernadac, A., Zhang, M., Chanal, A., Ize, B., Blanco, C., and Wu, L. F. (2001) Translocation of jellyfish green fluorescent protein via the Tat system of *Escherichia coli* and change of its periplasmic localization in response to osmotic up-shock, *J. Biol. Chem. 276*, 8159−64.
21. Thomas, J. D., Daniel, R. A., Errington, J., and Robinson, C. (2001) Export of active green fluorescent protein to the periplasm by the twin-arginine translocase (Tat) pathway in *Escherichia coli*, *Mol. Microbiol. 39*, 47−53.
22. Brüser, T., and Sanders, C. (2003) An alternative model of the twin arginine translocation system, *Microbiol. Res. 158*, 7−17.
23. Asai, T., Shinoda, Y., Nohara, T., Yoshihisa, T., and Endo, T. (1999) Sec-dependent pathway and ΔpH-dependent pathway do not share a common translocation pore in thylakoidal protein transport, *J. Biol. Chem. 274*, 20075−8.
24. Musser, S. M., and Theg, S. M. (2000) Characterization of the early steps of OE17 precursor transport by the thylakoid ΔpH/Tat machinery, *Eur. J. Biochem. 267*, 2588−98.
25. Cline, K., and Mori, H. (2001) Thylakoid ΔpH-dependent precursor proteins bind to a cpTatC−Hcf106 complex before Tha4-dependent transport, *J. Cell Biol. 154*, 719−29.
26. Brüser, T., Yano, T., Brune, D. C., and Daldal, F. (2003) Membrane targeting of a folded and cofactor-containing protein, *Eur. J. Biochem. 270*, 1211−21.
27. San Miguel, M., Marrington, R., Rodger, P. M., Rodger, A., and Robinson, C. (2003) An *Escherichia coli* twin-arginine signal peptide switches between helical and unstructured conformations depending on the hydrophobicity of the environment, *Eur. J. Biochem. 270*, 3345−52.
28. Van Voorst, F., and De Kruijff, B. (2000) Role of lipids in the translocation of proteins across membranes, *Biochem. J. 347* (Part 3), 601−12.
29. Martoglio, B., Hofmann, M. W., Brunner, J., and Dobberstein, B. (1995) The protein-conducting channel in the membrane of the endoplasmic reticulum is open laterally toward the lipid bilayer, *Cell 81*, 207−14.

BI052188A